Dual-Readout Calorimetry for High-Quality Energy Measurements

Progress Report

Presented by:

Dr. Richard Wigmans[1]

on behalf of the RD52 (DREAM) Collaboration

14 April 2015

[1]Contact person. Tel. [806] 834 6283, FAX [806] 742 1182, E-mail: wigmans@ttu.edu

1 Introduction

On August 31, 2011, the CERN Research Board decided to accept the DREAM Collaboration's detector R&D proposal [1] and included it as project RD52 in its official scientific program. This document constitutes the fourth RD52 progress report. In this report, we describe our activities since the last time we reported to the SPS Committee (April 8, 2014 [2]), as well as our future plans.

Recently, the SPS was restarted after a long shutdown. At the end of 2014, we were allocated 6 days of beam time in our usual location at the end of the H8 beam line. We used this time to collect some new data with the two fiber calorimeters described in our previous annual SPSC report. The first paper resulting from these beam tests will soon be submitted for publication, and we have started working on the analysis of data that will most likely result in a second publication. We have also continued our elaborate program of Monte Carlo simulations of the performance of the unusual calorimeters that are the topic of our studies. A paper on some of these results [3] was published in the past year. All this progress is in large part thanks to the tireless efforts of Dr. Sehwook Lee, one of the most dedicated members of our collaboration.

We are in the process of preparing for a new round of experimental data taking in 2015, using our existing calorimeters. New copper based calorimeter modules are about to be constructied in Ames, Iowa. We are planning to build a calorimeter consisting of 4×4 copper based modules, containing 64 towers and thus producing 128 signals for each event. Proper testing of this instrument (which involves calibrating 128 photomultiplier tubes with an electron beam) will require an uninterrupted test beam period of at least two weeks.

In the past year, the latest RD52 results have been presented at a number of colloquia and seminars. They were also featured at the CALOR 14 conference in Giessen (Germany), as well as at the Bethe forum in Bonn. The talks, as well as all publications in the context of this project, can be found at the RD52 website:
http://highenergy.phys.ttu.edu/dream/results/talks/talks.html

Details about our various past, current and planned activities are given in the next sections.

2 New results

Since the results from our 2012 test beam campaigns were all published, and no new experimental data were available until the end of 2014, a lot of effort has been spent on an elaborate program of Monte Carlo simulations of our, in many ways, very unusual calorimeters. The purpose of these simulations, based on GEANT4, was twofold:

1. To test the (limits of the) validity of such simulations with experimental data already obtained. In particular, we were interested in the dependence of the response function and the energy resolution on parameters such as the particle's energy and its angle of incidence.

2. To predict the effects on the performance for certain modifications of the detectors, for example a larger instrumented mass, an increased light yield, or a different choice of absorber medium.

The first results of this work have been summarized in the following publication:

- *Lessons from Monte Carlo simulations of the performance of a dual-readout fiber calorimeter*,
  N. Akchurin *et al.*, Nucl. Instr. and Meth. in Phys. Res. **A762** (2014) 100 - 118.

A selection of the results of this work, which consumed a few thousand CPU hours on the computer systems at our disposal, was shown in last year's report to the SPSC.

2.1 The calorimeter performance for electromagnetic showers

For em showers, the Monte Carlo simulations predicted some very specific effects that would occur for very small angles of incidence. These predictions included:

1. A dip in the calorimeter response when the angle of incidence in the vertical plane (θ) would be the same as the angle of incidence in the horizontal plane (ϕ).

2. A deterioration of the em energy resolution for very small angles of incidence.

3. An electron resolution for the sum of the scintillation and Čerenkov signals that is significantly better, by more than a factor of $\sqrt{2}$, than the resolution measured for either of the two types of signals individually.

4. An anti-correlation between the signals measured with the scintillating fibers and the signals measured with the Čerenkov fibers.

The first effect would be due to the fact that when $\theta = \phi$, the shower axis may penetrate over great depth inside the calorimeter without encountering a single fiber. The other effects derive from the fact that the early component of em showers (*i.e.* before the shower maximum is reached) is extremely collimated. When an electron enters this calorimeter parallel to the fibers, then the signal from the early shower component strongly depends on the impact point, *i.e.* inside a fiber or in between fibers. This leads to a deterioration of the em energy resolution and may also affect the calorimeter response.

Verification of these predictions was a major purpose of the program of beam tests we carried out in the few days allocated to RD52 in December 2014. The data obtained during these tests have been analyzed and the results are described in a new paper that will be submitted for publication, once the specific Monte Catlo simulations pertaining to these tests have been completed:

- *The small-angle performance of a dual-readout fiber calorimeter*,
  A. Cardini *et al.*, to be submitted to Nucl. Instr. and Meth. in Phys. Res. .

In the following, we show some of the results of these studies, which greatly benefitted from the fact that the CERN people responsible for the SPS beam lines (I. Efthymiopoulos and his crew, especially M. Jeckel) equipped the table on which our calorimeter is installed with a mechanism that allowed us to rotate it in the horizontal plane with milliradian precision and reproducibility. These studies were all carried out with a beam of 20 GeV positrons. This energy was chosen

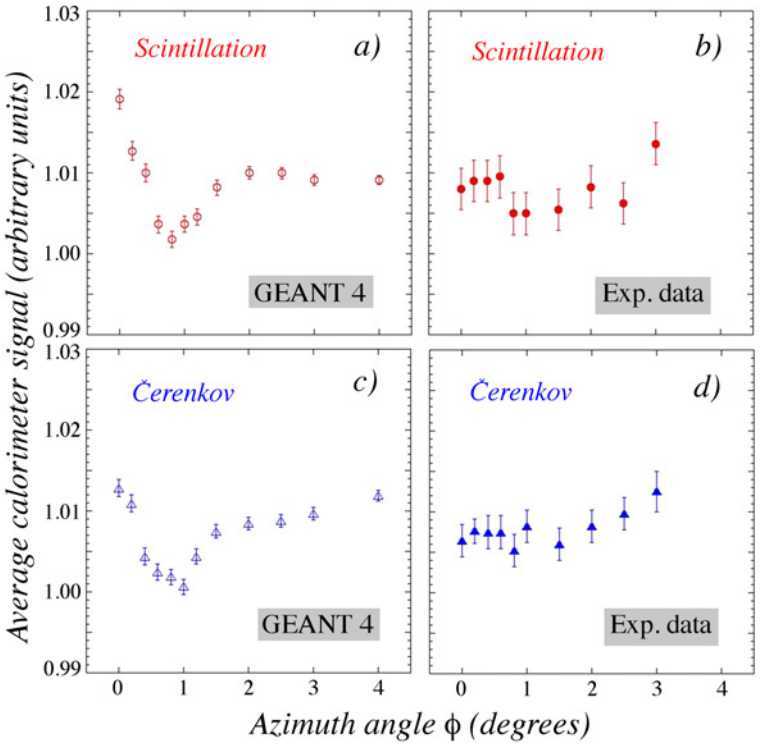

Figure 1: Comparison between the measured calorimeter response (b, d) and the GEANT4 prediction (a, c), as a function of the azimuth angle ϕ, for a tilt angle $\theta = 1^\circ$. Results are given separately for the scintillation (a, b) and Čerenkov (c, d) signals.

because the calorimeter performance at this energy is dominated by stochastic fluctuations. In Figure 1, the measured response is shown together with the GEANT4 prediction[1], as a function of the azimuth angle of incidence ϕ, for a tilt angle $\theta = 1^\circ$. The clear dip predicted by the Monte Carlo simulations for $\phi = \theta = 1^\circ$ is experimentally *not* observed, neither for the scintillation signal nor for the Čerenkov one. The predicted dip at $\phi = 2^\circ$ for the measurement at a tilt angle $\theta = 2^\circ$ is not observed experimentally either. Even though the predicted effects are small, the decrease of the response by 1.5 - 2% between $\phi = 0$ and $\phi = 1(2)^\circ$ is experimentally ruled out at a confidence level $> 99\%$.

Contrary to the calorimeter response, which was very constant as the angle of incidence of the electrons was varied, the energy resolution turned out to be strongly dependent on that angle, at least for the scintillation signals. This is illustrated in Figure 2, which shows the energy resolution as a function of the azimuth angle of incidence ϕ, for a tilt angle $\theta = 1^\circ$.

The figure shows remarkable differences between the two types of signals. Not only is the energy resolution significantly worse for the scintillation signals, for all angles in this range, but the resolution measured for the scintillation signals also depends strongly on the angle of incidence, unlike the resolution measured with the Čerenkov signals.

These results are consistent with earlier observations that the energy resolution at a fixed angle of incidence ($\phi = 1.5^\circ, \theta = 1.0^\circ$) tends to become better for the Čerenkov signals than

[1]It should be pointed out that this prediction concerned the RD52 calorimeter made with lead absorber [3].

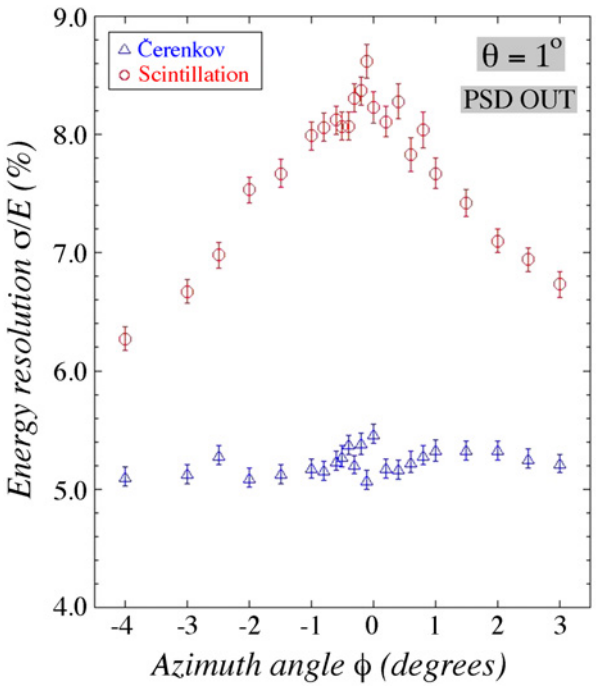

Figure 2: The energy resolution measured for 20 GeV electrons in the scintillation and the Čerenkov channels, as a function of the azimuth angle of incidence (ϕ) of the beam particles. The tilt angle θ was 1°.

for the scintillation ones as the energy of the electron beam increases [4]. Since the sampling structure is the same for both types of fibers, and the light yield considerably larger (and event-to-event fluctuations in the number of scintillation photoelectrons thus correspondingly smaller), one would naively expect to measure better energy resolutions for the scintillation signals. The fact that the opposite effect is experimentally observed is a consequence of the extremely collimated nature of the em showers in the early stage of the shower development, before the shower maximum is reached, *i.e.* in the first 10 cm of this particular calorimeter.

Neighboring fibers *of the same type* are separated by 2 - 3 mm and that distance is of the same order as the shower width in this early stage of the shower development. Therefore, the calorimeter signal (from this early shower component) depends crucially on the impact point of the particles, if these enter the calorimeter parallel to the fibers. This dependence is quickly reduced when the particles enter the calorimeter at a small angle with the fibers. For example, at 2° the lateral displacement over a depth of 10 cm already amounts to 3.5 mm, comparable with the fiber-to-fiber distance. As the angle increases, this early collimated shower component is thus sampled more and more in the same way as the rest of the shower. However, at angles where this is not the case, this effect adds an additional component to the em energy resolution. This effect is, in first approximation[2], energy independent and thus acts as a constant term.

Now, why does this effect only affect the resolution measured with the scintillation signals? The reason is that the collimated early shower component does *not* contribute to the Čerenkov

[2]The depth of the shower maximum increases with the shower energy, but this is a logarithmic effect. For example, the shower maximum for 10 GeV electrons in copper is located at $\sim 5X_0$, and for 100 GeV at $\sim 8X_0$.

signals, since the Čerenkov light produced by shower particles traveling in the same direction as the fibers falls outside the numerical aperture of the fibers. Another spectacular consequence of this phenomenon is the fact that calorimeters of this type can distinguish event-by-event between the energy loss in the form of ionization and radiation when detecting muons, since the Čerenkov fibers only produce signals for the bremsstrahlung component [5]. For the 20 GeV electrons, the Čerenkov fibers thus only register shower particles that travel at relatively large angles with the shower axis ($20 - 60°$), and such particles are for all practical purposes only found beyond the shower maximum, where the shower is wide compared to the typical distance separating neighboring fibers of the same type. The "constant" term that affects the scintillation resolution is thus practically absent for the Čerenkov signals.

It turns out that the effect that causes the difference between the angular dependence of the two types of calorimeter signals is extremely sensitive to the presence of an upstream absorber (see Figure 3). We noticed this from the effects of the preshower detector (PSD), a $1X_0$ lead absorber followed by a plastic scintillator plate that served to identify pions contaminating the electron beam. The energy resolution measured with the Čerenkov signals deteriorates when

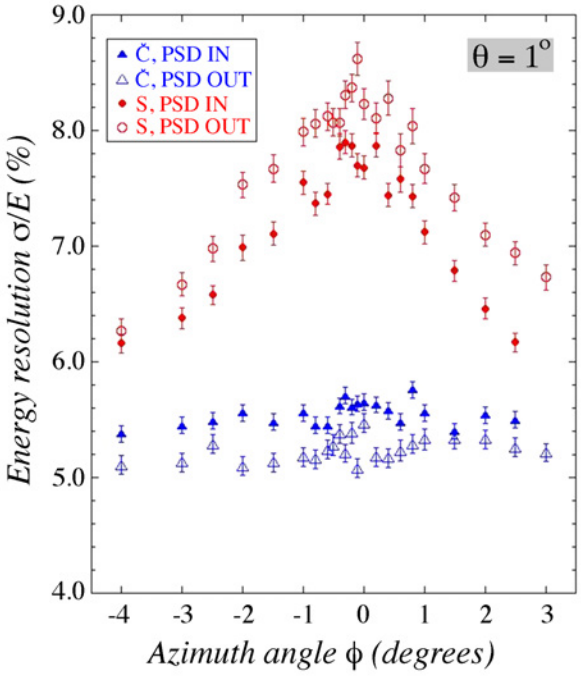

Figure 3: The energy resolution measured for 20 GeV electrons in the scintillation and Čerenkov channels, as a function of the azimuth angle of incidence (ϕ) of the beam particles. Results are compared for data taken with and without the preshower detector in the beam line. The tilt angle θ was $1°$ in both cases.

the PSD is in the beam line. This is to be expected, since the fluctuations that determine the energy resolution of the calorimeter are now increased because of the additional fluctuations in the amount of energy absorbed by this upstream device. Surprisingly, the energy resolution measured with the scintillation signals exhibits the opposite effect, it *improves* as a result of installing the $1X_0$ thick absorber upstream of the calorimeter. This effect is a consequence of the

fact that the absorber causes the shower to start effectively 80 cm upstream of the calorimeter proper. As a result, upon entering the calorimeter, the shower is somewhat less radially collimated than when the beam particles enter the calorimeter undisturbed. Therefore, the impact point dependence of the calorimeter response is somewhat reduced, and it is this impact point dependence that is responsible for the fact that the scintillation resolution is so much worse for the scintillation signals than for the Čerenkov ones, at very small angles of incidence.

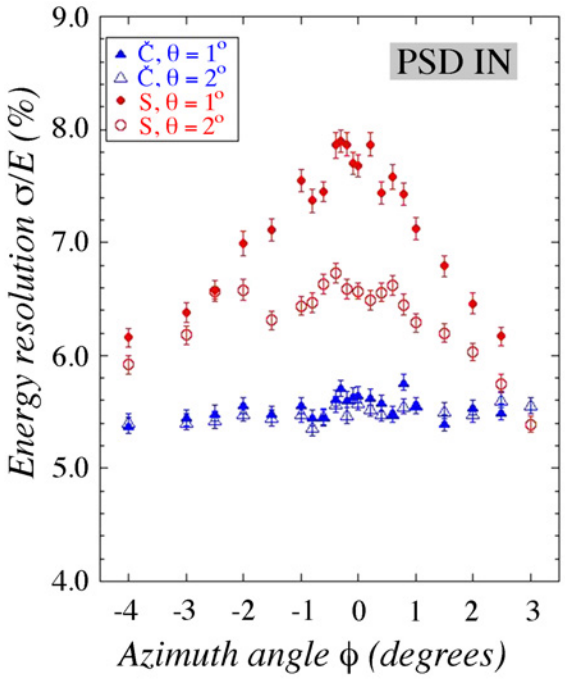

Figure 4: The energy resolution measured for 20 GeV electrons in the scintillation and the Čerenkov channel, as a function of the azimuth angle of incidence (ϕ) of the beam particles. Results are compared for tilt angles θ of 1° and 2°. These results were obtained with the PSD in the beam line.

We also investigated the effect of the tilt angle θ (Figure 4). It turns out that by increasing this angle from 1° to 2°, the angular dependence of the resolution in the scintillation channel is substantially reduced, while it is of course no surprise that this has no effect on the resolution measured in the Čerenkov channel.

The use of two independent signals in dual-readout calorimeters is inspired by the beneficial effects of measuring the em shower component event by event for the *hadronic* calorimeter performance. For the detection of em showers, initiated by electrons or photons, there is absolutely no compelling reason to consider these signals separately. Both types of fibers sample the em showers independently and, as illustrated by the results shown in Figures 2 and 4, the Čerenkov signals provide an even better energy resolution for small angles of incidence, despite the considerably smaller light yield. There is thus absolutely no reason why one should not use the combination of both signals to measure the properties of the showering electrons or photons. Since the sampling fraction and the sampling frequency are twice as large as for the two individual channels, one should expect the contribution of sampling fluctuations to the energy resolution to be reduced by as much as a factor of $\sqrt{2}$. In addition, the much smaller effective

fiber-to-fiber distance should reduce the angular dependence of the energy resolution.

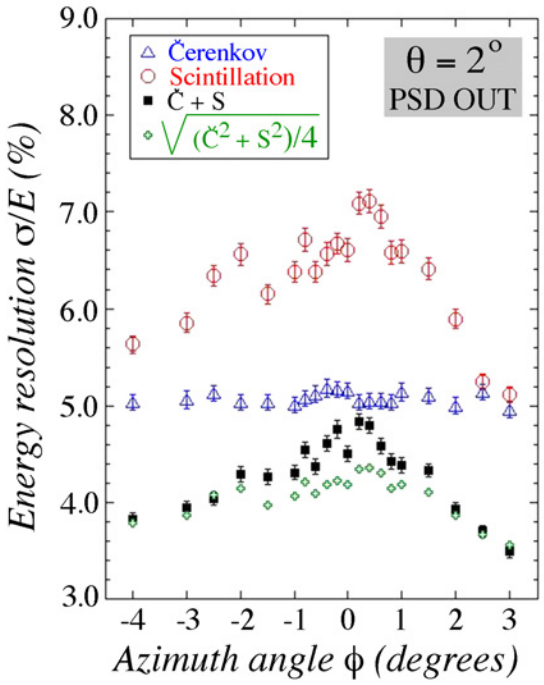

Figure 5: The energy resolution measured for 20 GeV electrons in the scintillation and the Čerenkov channels and for the sum of both signals, as a function of the azimuth angle of incidence ϕ. The tilt angle θ was 2° and the PSD was out of the beam line.

Figure 5 shows the energy resolution for the 20 GeV electron showers for the sum of the scintillation and the Čerenkov signals, as a function of the azimuth angle of incidence ϕ. For comparison, the results measured for the two signals separately are shown as well. The results qualitatively confirm the naive expectation formulated above. Using the sum of both signals, the energy resolution is found to be better than for the individual signals, and less dependent on the angle of incidence than the resolution measured with the scintillation signals. This is good news, since it means that the dual-readout fiber calorimeter is not only an excellent hadron calorimeter, but also provides good performance for em showers. This distinguishes this detector from compensating calorimeters such as the ZEUS [6] and SPACAL [7] ones, where the em energy resolution was dominated by sampling fluctuations, which were large because of the requirement of a small sampling fraction.

The em energy resolution for each of the two signals is determined by sampling fluctuations and by fluctuations in the number of photoelectrons. Apart from these stochastic fluctuations, there is also an angle dependent constant term which only contributes to the scintillation resolution. Because of the structure of the calorimeter, the sampling fluctuations are the same for both types of signals, and if these were the only contribution to the energy resolution, then one would expect the resolution to be smaller by a factor of $\sqrt{2}$ for the combined signal. If photoelectron statistics would only affect the Čerenkov resolution, and the constant term only the scintillation

resolution, one can show that the resolution for the combined signals is equal to

$$\frac{\sigma_{[C+S]/2}}{E} = \frac{\sqrt{(\sigma_C/E)^2 + (\sigma_S/E)^2}}{2} \quad (1)$$

The (green) crosses in Figure 5 represent the result of this calculation. They describe the measured resolution very well for angles $\phi \geq 2°$.

The fact that the energy resolution in the Čerenkov channel is 5% leads immediately to the conclusion that this signal must consist of at least 400 photoelectrons (20 Cpe/GeV). If we include the contributions of sampling fluctuations, which may be estimated at 2.8% [8], we find a Čerenkov light yield of 30 Cpe/GeV (*i.e.* 600 photoelectrons for 20 GeV showers). Sampling fluctuations also contribute 2.8% to the energy resolution for the scintillation channel. Therefore, the constant term deriving from the impact point dependence of the response clearly dominates this resolution, for all angles of incidence studied here. However, by combining the Čerenkov and scintillation signals, the value of this constant term drops below 2% for angles of incidence larger than 2 degrees. This is consistent with our previous findings [4].

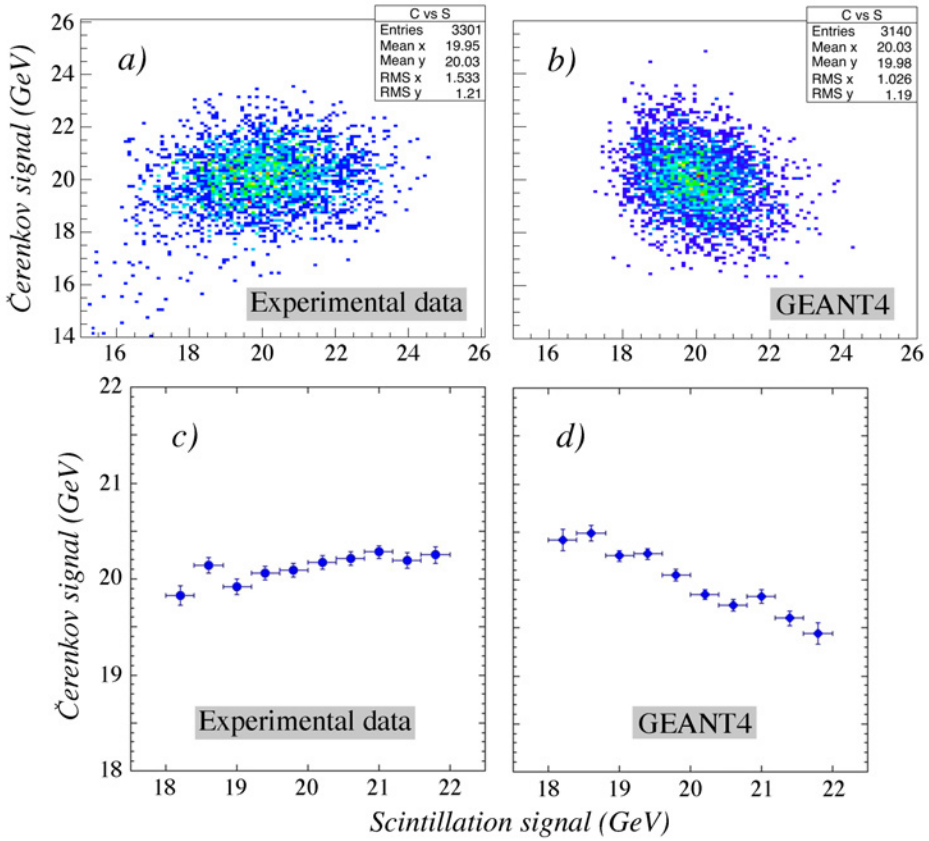

Figure 6: Scatter plots of the Čerenkov versus the scintillation signals for 20 GeV electrons in the RD52 copper dual-readout calorimeter. Experimental data (a) are compared with GEANT4 simulations (b). Also shown are the average Čerenkov signals as a function of the average scintillation signal, measured in slices with a width of 0.4 GeV (c, d). The angle of incidence of the beam particles was ($\phi = 1.5°, \theta = 1.0°$).

We are in the process of comparing the measured angular dependence of the em energy resolution of our calorimeter with the predictions of the GEANT4 simulations. Unfortunately, these simulations require a lot of CPU time and therefore this is a slow process. At the present time, the Monte Carlo results are still preliminary and incomplete. However, there is one interesting GEANT4 prediction that has been reconfirmed for our copper structure and which is illustrated in Figure 6.

The position dependence of the scintillation signal that is the cause of the angular dependence of the scintillation resolution (Figure 2) implies a larger signal when the beam particle enters the calorimeter inside a scintillating fiber than at a position in between two scintillating fibers. Effects 3 and 4 listed at the beginning of this section are closely related, since the GEANT4 simulations predict the same effect for the Čerenkov signals. In other words, when the scintillation signal reaches its maximum value, the Čerenkov signal is at its minimum. This anti-correlation between the two types of signals is clearly visible in the scatter plot shown in Figure 6(b,d). It is also responsible for a strong improvement in the energy resolution when both signals are combined.

However, the predicted anti-correlation is *not* confirmed by the measurements. The experimental data shown in Figures 6(a,c) are clearly at variance with the GEANT4 results. The absence of an anti-correlation between the two experimental signals should not really be a surprise, since the strong angular dependence of the calorimeter resolution observed for the scintillation signals was found to be absent for the Čerenkov signals (Figures 2 - 4). Since this angular dependence is a direct consequence of the impact point dependence of the calorimeter response, there is thus no reason for an anti-correlation between the two signals.

2.1.1 Time structure measurements

A second part of our measurements in 2014 concerned the time structure of the signals provided by our dual-readout fiber calorimeters. We used the 36-tower lead-fiber calorimeter for this purpose. This calorimeter was also surrounded by a set of 20 leakage counters, blocks of plastic scintillator with dimensions $50 \times 50 \times 10$ cm^3. In total, 30 different signals were read out with a CAEN V1742 switched capacitor digitizer, based on the DRS4 chip. This device provided 5 Gs/s digitization of these signals.

The analysis of these data has just started, but we would like to show some examples of the preliminary results. These results concern a 40 GeV positive beam, which consisted of a mixture of electrons, pions and muons. The different particles were identified with external counters, *i.e.* the preshower detector, a tail catcher and the muon counter. The following plots show the average time structures for a few thousand particles of each type. In order to appreciate these figures, one should realize that the light produced in the fibers travels at a slower speed (c/n, with $n \sim 1.5$) than the particles that generate the light.

Figure 7 shows the average time structure of the Čerenkov signals from the calorimeter tower into which the beam particles were steered. The muons produce light over the full 2.5 m length of the calorimeter module, and therefore the signals start earlier than for the electrons and pions. The shower maximum for the pions is located deeper inside the calorimeter than for electrons, and therefore the pion signals also start earlier. Figure 8 shows a comparison between the Čerenkov and scintillation signals measured in the same calorimeter tower, for electron (Fig.

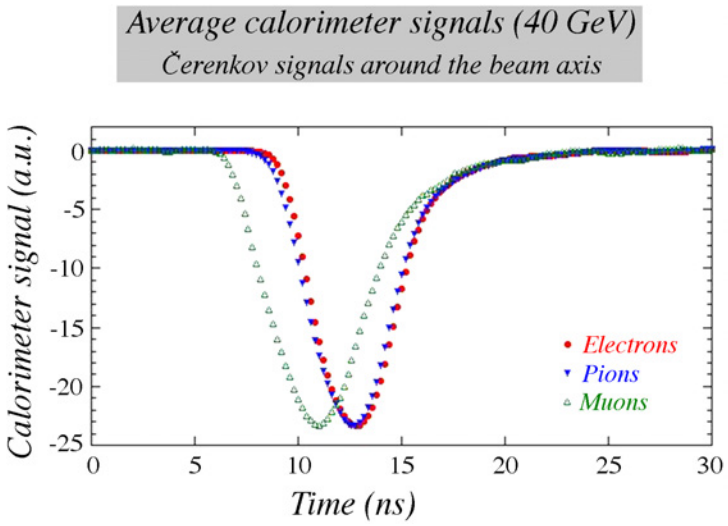

Figure 7: Typical Čerenkov signals measured for 40 GeV electrons, pions and muons in the tower into which the beam particles were steered. See text for more details.

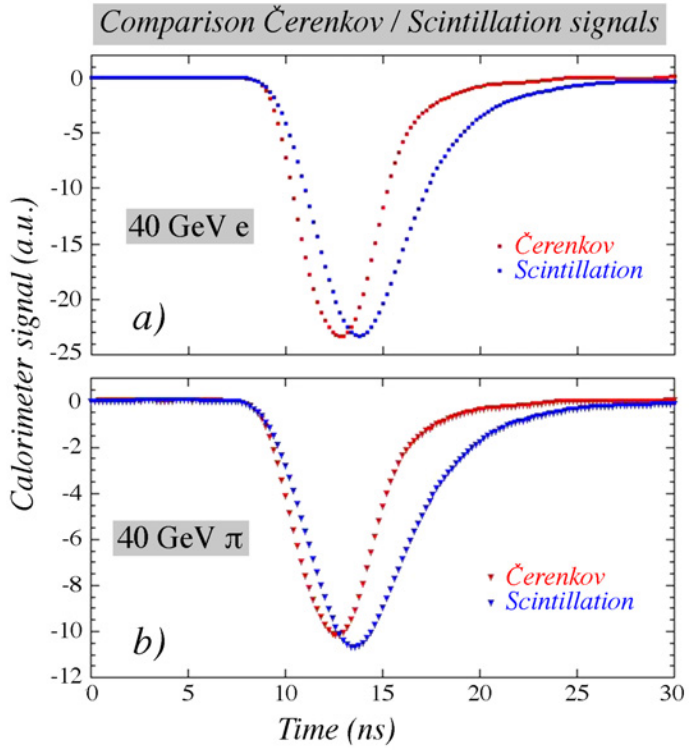

Figure 8: Comparison between the Čerenkov and scintillation signals measured for 40 GeV electrons (a) and pions (b) in the tower into which the beam particles were steered. See text for more details.

8a) and pion (Fig. 8b) showers. The electron signals illustrate the difference resulting from the fact that the Čerenkov signals are prompt, while the scintillation ones are affected by the decay of the scintillating fluors. The pion signals illustrate, in addition, the fact that there is

relatively less Čerenkov light produced (because of the contribution of nonrelativistic shower particles to the scintillation signals), and the related fact that the Čerenkov light is produced in a longitudinally more restricted area than the scintillation light.

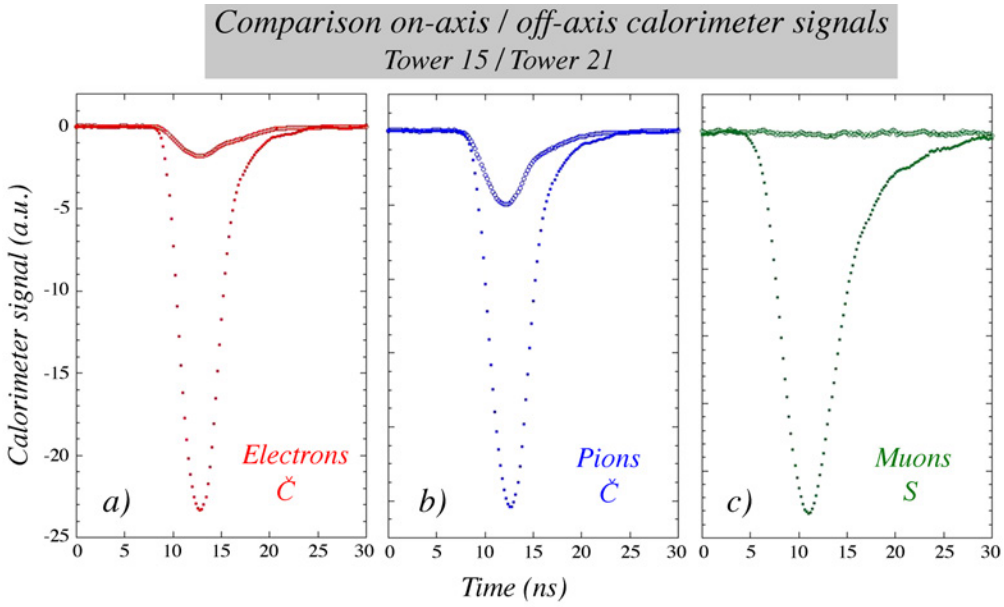

Figure 9: Comparison between the calorimeter signals produced in a tower that contains the shower axis and in a neighboring tower. Results are shown for 40 GeV electrons (a), pions (b) and muons (c). See text for more details.

In Figure 9, the signals measured in the tower that contains the shower axis and in a neighboring tower are compared, for 40 GeV electrons (Fig. 9a), pions (Fig. 9b) and muons (Fig. 9c). The figure shows that the muon signals are limited to the tower traversed by the beam particles. Also the electrons deposit most of their energy in this tower, while hadron showers are clearly more extended in the lateral direction.

The pion component of the beam was also completely responsible for any signals recorded by the leakage counters. Figure 10 shows the average signals recorded in two different leakage counters. These counters were located close to the shower maximum (the red signal), and near the end of the calorimeter module (the blue signal). The latter signal consisted very likely exclusively of recoil protons produced by elastic neutron scattering, while the red signal may also contain a contribution from charged particles produced in the shower development and escaping the calorimeter. In the hadronic shower development, typically a few thousand neutrons are released from the nuclei in which they were bound. They typically carry a few MeV kinetic energy and lose that energy predominantly by means of elastic scattering, with a time constant of ~ 10 ns [8]. The time difference between the two signals shown in Fig. 10 and the difference in rise time are consistent with the above assessment. We expect to be able to extract much more information out of these data than shown here. We are also planning follow-up measurements with a much faster light detector (see Section 3).

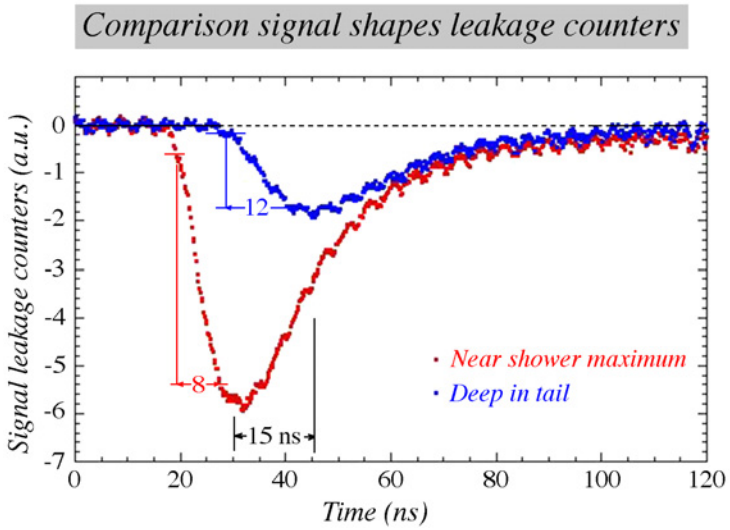

Figure 10: Comparison between the signals produced by 40 GeV pions in two of the leakage counters surrounding the RD52 lead-fiber calorimeter. See text for more details.

2.2 The hadronic calorimeter performance

It is quite likely that the discrepancies observed between the experimental data and the Monte Carlo simulations described in the Section 2.1.1 are a consequence of the intricacies of the calorimeter structure. Perhaps, specific issues related to the generation of Čerenkov light in the optical fibers play a role as well. The fine details of calorimeter structure should pose less of a problem for hadron showers. Whereas the signal from an em shower depends crucially on the contribution of one single fiber, which may be smaller or larger depending on the precise trajectory of the incoming particle, the signals from hadronic showers are typically composed of the combined contributions of hundreds to thousands of different fibers.

In our previous SPSC report, we showed that "standard" hadronic shower simulations gave a reasonable description of the response functions for 100 GeV π^- in the original DREAM copper-fiber calorimeter. Especially the Čerenkov response function was well described by these simulations. On the other hand, the scintillation distribution was more narrow, less asymmetric and peaked at a lower value than for the experimental data. We also found that the hadronic signal non-linearity, which is typical for every non-compensating calorimeter, was much better described for the Čerenkov signals than for the scintillation ones. From additional analyses, we established that the non-relativistic component of the shower development, which is completely dominated by processes at the nuclear level, is rather poorly described by GEANT4, at least by the FTFP_BERT hadronic shower development package, which is the standard used by the ATLAS and CMS collaborations. Both the average size of this component, as well as its event-to-event fluctuations, are at variance with the experimental data. This non-relativistic shower component only plays a role for the scintillation signals, *not* for the Čerenkov ones.

Yet, some aspects of hadronic shower development that are important for the dual-readout application were found to be in good agreement with the experimental data. As examples, we mention the shape of the Čerenkov response function and the radial shower profiles. Attempts

to use the dual-readout technique on simulated shower data reasonably reproduced some of the essential characteristics and advantages of this method: a Gaussian response function, hadronic signal linearity and improved hadronic energy resolution. The fact that the reconstructed beam energy was systematically too low may be ascribed to the problems with the non-relativistic shower component mentioned above.

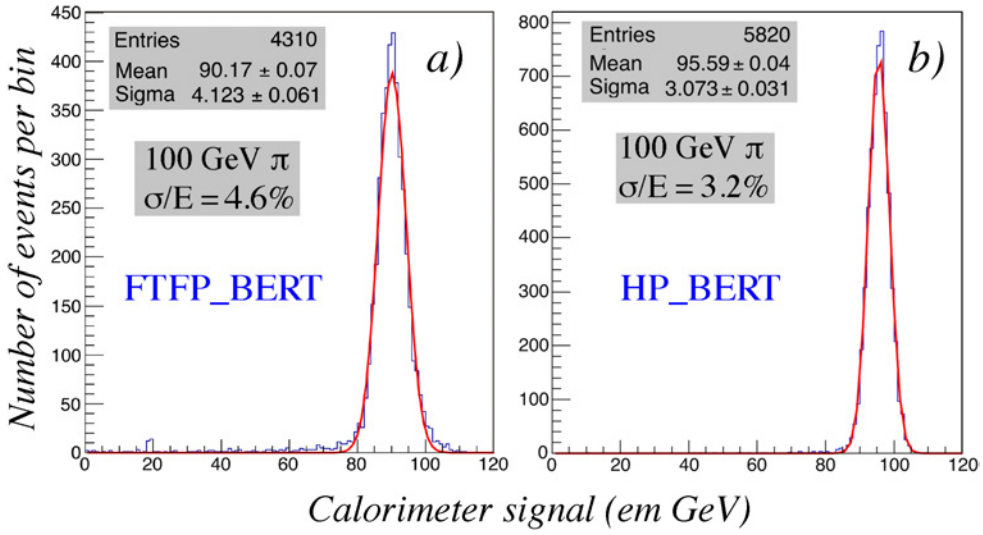

Figure 11: The response function for 100 GeV pions in a dual-readout fiber calorimeter based on copper absorber. Results of GEANT4 Monte Carlo simulations, using the FTFP_BERT (a) or the HP_BERT (b) hadron shower development package.

An important reason for performing these very time consuming simulations was to see if and to what extent the hadronic performance would improve as the detector size is increased. Figure 11a shows the signal distribution obtained for 100 GeV π^- in a copper based RD52 calorimeter with a lateral cross section of 65×65 cm^2. The mass of such a ($10\lambda_{\rm int}$ deep) device would be ~ 6 tonnes. According to these simulations, which were carried out with the FTFP_BERT package, the average calorimeter signal, reconstructed with the dual-readout method, would be 90.2 GeV, and the energy resolution would be 4.6%.

In order to see to what extend these simulations depend on the choice of the hadronic shower development package, we repeated these simulations using the high precision version of the hadronic shower simulation package (HP_BERT), which seems to provide a much more elaborate treatment of the numerous neutrons produced in the shower process, but also takes an order of magnitude more CPU time. Figure 11b shows the results of this work, which took about 20 minutes of CPU time per event. And indeed, the results show a clear improvement: the average calorimeter signal has increased to 95.6 GeV, and is thus within a few percent equal to that of an em shower developing in the same calorimeter structure (one of the crucial advantages of calorimeters based on the DREAM principle). Also the energy resolution has significantly improved, from 4.6% to 3.2%.

We also generated 4630 events for 200 GeV with the HP_BERT package. This gave an average signal of 191 GeV and an energy resolution of 2.4%. The results of the various simulations

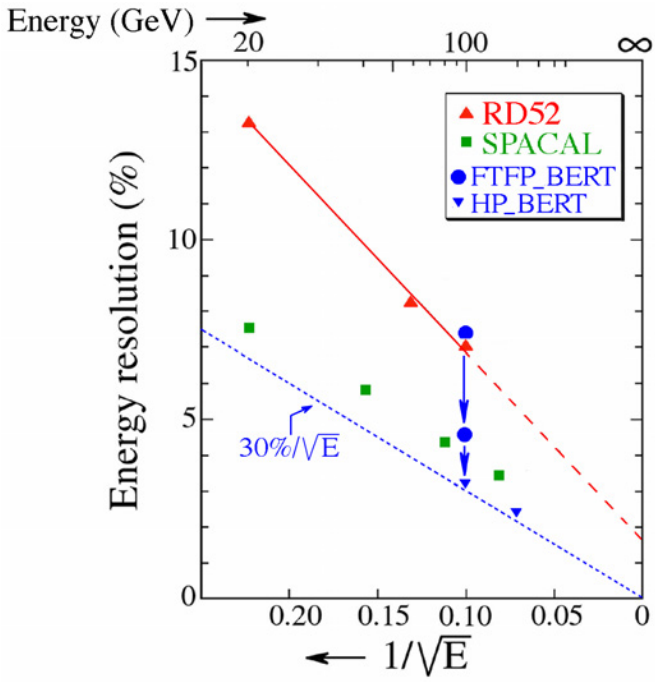

Figure 12: The energy resolution for single pions measured with the dual-readout RD52 [9] calorimeter. For comparison, the record resolutions reported for the SPACAL calorimeter are shown as well [7]. Also shown are the results of GEANT4 simulations for the current and full-size RD52 copper-fiber calorimeter, using the FTFP_BERT hadronic shower package [3], as well as the results obtained with the HP_BERT package for the full-size copper-fiber calorimeter [10].

are summarized in Figure 12.

Figure 12 summarizes the situation concerning the hadronic energy resolution, for single pions. It shows experimental data obtained with the RD52 calorimeter, as well as the record setting results published by SPACAL [7]. Also shown are the GEANT4 predictions for a 3×3 and 7×7 module RD52_Cu calorimeter, obtained with the FTFP_BERT package [3], as well as the HP_BERT predictions for 100 and 200 GeV pions. The latter are well described by the dotted line, which corresponds to a resolution of $30\%/\sqrt{E}$.

We believe that the predicted improvement in the performance resulting from an increased detector size is realistic. The resolution of the instruments tested so far was clearly dominated by leakage fluctuations. An increase in the detector volume would reduce the effects of this, in which case resolutions of a few percent seem to be feasible, and would bring the hadronic performance of the RD52 calorimeter at the same level as that of the compensating SPACAL and ZEUS calorimeters, or even better. The potential importance of this is illustrated in Figure 13, which shows the results of the simulation of a mixture of hadron showers with energies corresponding to the masses of the W and Z bosons. The two peaks are clearly separated, which is a design requirement for calorimeters at future e^+e^- colliders. Of course, just like with all other hadron calorimeter results, these simulations need to be verified experimentally in order to establish how realistic they really are.

It should be emphasized that the results shown in Figures 11 - 13 are for *single hadrons*.

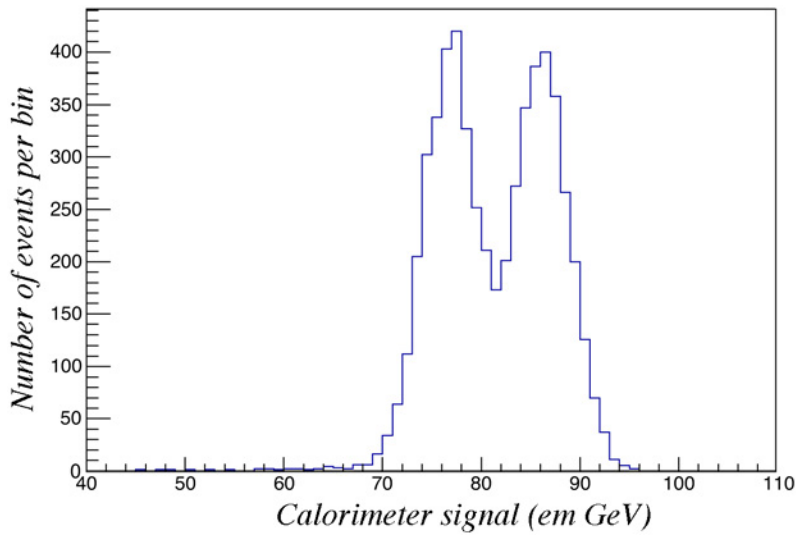

Figure 13: The response curve for a mixture of hadrons with energies corresponding to the W and Z masses. Results of simulations with the high precision GEANT4 package.

There is an important reason why the jet energy resolution of copper based dual-readout fiber calorimeters may also be expected to be much better than that of the high-Z compensating calorimeters [11]. A sizable component of the jet consists of soft hadrons, which range out rather than developing showers. The response of calorimeters such as ZEUS to these particles is considerably larger than the response to the showering γs and high-energy hadrons. The scale for the difference between these responses is set by the e/mip value, which was measured to be 0.62 in ZEUS and 0.72 in SPACAL. The advantage of an absorber material with much lower Z is an e/mip value that is much closer to 1 (the value at which point this effect ceases to play a role). For our copper based dual-readout fiber calorimeter, an e/mip value of 0.84 was found.

The possibility to measure jets with superior resolution compared to previously built high-Z compensating calorimeters was one of the main reasons why we embarked on the dual-readout project.

3 Future plans

The DREAM/RD52 Collaboration has a very solid record of turning SPS beam time combined with limited funding into high-quality, well-regarded publications. So far, this project has resulted in 27 papers in the journal Nuclear Instruments and Methods in Physics Research, with two additional papers in preparation [12]. There is also no shortage of new ideas to further investigate the possibilities and limitations of this exciting new calorimeter concept and to optimize applications in practical detectors based on its principles. Yet, we have to face the reality that it is exceedingly difficult to obtain financial support for this type of generic detector R&D. Until now, our main sources of funding have been the US Department of Energy, through a special program for Advanced Detector Research, and INFN in Italy. However, both funding streams have dried up, because of limited resources and shifting priorities within the funding agencies.

For this reason, the RD52 Collaboration has now been reduced to a "coalition of the willing", a group of researchers who have been involved in the project since a long time, and who enjoy working with each other on exciting and rewarding research, in some cases at great personal expense and sacrifice. This new situation implies that we have to be realistic concerning the long-term plans outlined in last year's progress report [2]. Development of higher-density and projective absorber structures, as well as alternative readout systems based on SiPMs will require substantial amounts of new money, and will be put on a backburner.

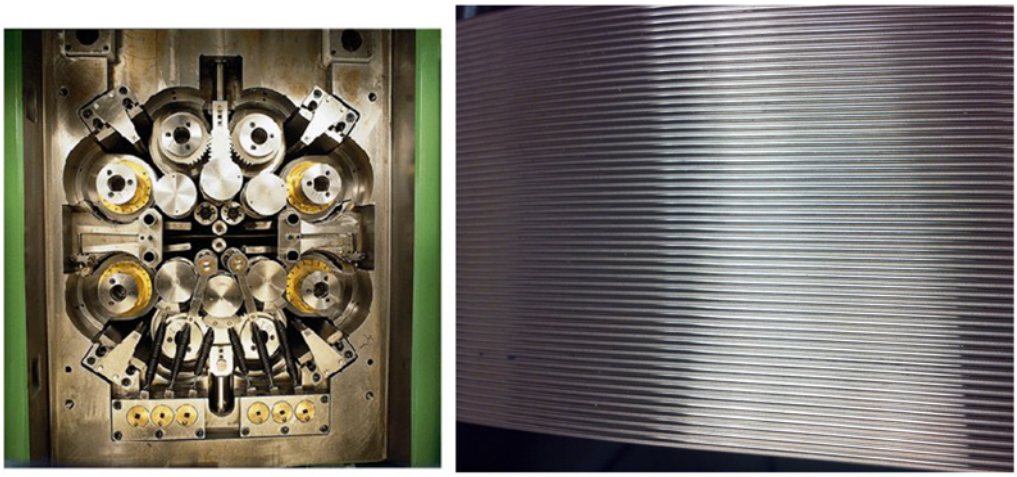

Figure 14: The rollers with which PMX produces grooved copper sheets for the RD52 project (a) and a sample of the result of this procedure (b).

One of the most challenging aspects of building this type of calorimeter is the problem of how to get very large numbers of optical fibers embedded in a uniform way in the metal absorber structure. Copper has turned out to be a particular difficult material to work with. We have tried many different ways, but so far only machining grooves in thin copper plates has provided the desired quality. The existing 120-kg maximum-fiber-density copper calorimeter was built this way. This very time consuming procedure is of course not applicable for mass production. Since one year, we are collaborating with one of the largest specialized factories in the world, PMX located in Cedar Rapids Iowa, in an attempt to manufacture grooved copper sheets with the required tolerances by means of rolling. The results are not yet ideal, but there has been steady improvement in successive trial runs. This part of the project is overseen by Professor Hauptman and colleagues at Iowa State University, together with the engineers of Ames National Lab. Figure 14 shows a sample from a recent trial run (Figure 14b), as well as the complicated roller with which this result was achieved (Figure 14a). This machine contains three banks of backup rollers.

We are hopeful that this work will soon lead to grooved copper sheets that meet the tight tolerances needed for the construction of a sizable calorimeter module. If that is the case, we will use our remaining funds to build the largest module we can afford, reusing the PMTs from the previous (current) generation of detectors. Professor Hauptman and his crew of ISU students are ready to take on this job, which will expectedly take about 6 months to complete. While

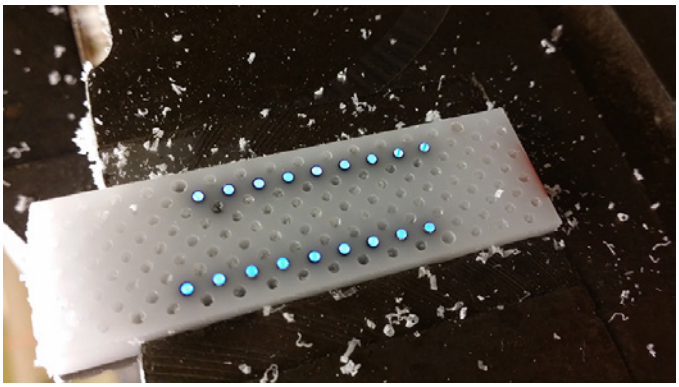

Figure 15: Milled off scintillating fibers which are used to test mirroring techniques at ISU.

waiting for the copper rolling to succeed, they have also carried out a variety of other projects intended to improve the optical quality of this new calorimeter. One such improvement concerns mirroring the upstream ends of the fibers, which will increase the light yield and the effective attenuation length of the fibers (Figure 15).

In the meantime, we are preparing for the August 2015 beam tests with a program based on our existing calorimeter modules. The time structure measurements carried out last December demonstrated the power of the DRS based time digitizers. We would like to take the precision level a step further and have purchased a number of MCP-PMTs, which convert the light into electrical signals that have a rise time of 0.2 ns, a pulse width of 0.7 ns and a transit time spread of only 35 ps. This should make it possible to extract more information than with the dynode based PMTs used so far, especially from the prompt Čerenkov signals. In particular, we hope that it will be possible to recognize the light reflected from the upstream aluminized ends of one of our copper modules as a separate (somewhat delayed) pulse. In that case, it would be possible to determine the depth at which the Čerenkov light is predominantly produced, with great precision.

We would also like to exploit the time structure of the signals to see to what extent it is possible to distinguish protons from pions. Differences between the showers induced by these particles are a consequence of the requirement of baryon number conservation, and the fact that a proton is a larger particle than a pion. As a result,

- The cross section for proton-induced nuclear reactions is larger, and the mean free path in the calorimeter is thus smaller than for pions.
- Proton induced showers are characterized by a leading baryon, which carries most of the transferred momentum in each subsequent generation of the shower develoment.
- Leading π^0s, which are quite common in the development of pion induced showers, are absent in proton showers. In proton showers, π^0s are only produced in non-leading processes. This manifests itself in a smaller average em shower component and smaller event-to-event fluctuations in the em shower component. Moreover, these fluctuations are more symmetric than for pion induced showers.

The latter effects, which all have been observed in practice [13], may also have unique measurable consequences in dual-readout calorimeters, and in particular also for the time structure of the events. Given the fact that the Čerenkov light is predominantly produced in the em showers generated by π^0s, the Čerenkov/scintillation signal ratio will typically be smaller for protons than for pions. In particular, it will be smaller near the shower axis. Looking at the Čerenkov signals, a time structure that indicates that a large amount of Čerenkov light is produced early in the shower development is most definitely ruling out a proton as the showering particle.

Finally, we would also like to properly assess the hadronic performance of the 36-tower 1350-kg lead fiber dual-readout calorimeter. Due to the very short beam period allocated to us in 2014, this part of the program had to be postponed. As anyone who has tested calorimeters in a systematic way in the North Area knows, it is very important to have control over the polarity and the energy of the beam particles that are sent into one's beam line. This is particularly true in H6/H8, which share beam particles from Target T4, and may have conflicting interests. We ask that the SPS Coordinator keeps this in mind when making the schedules, and discuss (and settle) any potential conflicts in a timely way with all parties involved.

References

[1] DREAM Collaboration (Wigmans R) 2010, CERN-SPSC-2010-012/SPSC-M-771.

[2] DREAM Collaboration (Gaudio G, Hauptman J and Wigmans R) 2014, CERN-SPSC-2014-010 ; SPSC-SR-135.

[3] Akchurin N *et al.* 2014, *Lessons from Monte Carlo simulations of the performance of a dual-readout fiber calorimeter*, Nucl. Instr. and Meth. in Phys. Res. **A762** (2014) 100 - 118.

[4] Akchurin N *et al.*, Nucl. Instr. and Meth. in Phys. Res. **A735** (2014) 130 - 144.

[5] Akchurin N *et al.*, Nucl. Instr. and Meth. in Phys. Res. **533** (2004) 305.

[6] Drews G *et al.*, Nucl. Instr. and Meth. in Phys. Res. **A290** (1990) 335.

[7] Acosta D *et al.*, Nucl. Instr. and Meth. in Phys. Res. **A308** (1991) 481.

[8] Wigmans R 2000, *Calorimetry, Energy Measurement in Particle Physics*, International Series of Monographs on Physics, Vol. 107, Oxford University Press.

[9] Wigmans R 2013, Nucl. Instr. and Meth. in Phys. Res. **A732** (2013) 475.

[10] Wigmans R *et al.*, *New results from the RD52 project*, Proc. of the 13th Int. Conf. "Frontier Detectors for Frontier Physics", Elba, 2015, to be published in Nucl. Instr. and Meth. in Phys. Res. .

[11] DREAM Collaboration (Wigmans R) 2012, CERN-SPSC-2012-014; SPSC-SR-100.

[12] http://highenergy.phys.ttu.edu/dream/results/publications/publications.html

[13] Akchurin N *et al.*, Nucl. Instr. and Meth. in Phys. Res. **A408** (1998) 380.